EXHBIT C

Temporally Distinct and Ligand-Specific Recruitment of Nuclear Receptor-Interacting Peptides and Cofactors to Subnuclear Domains Containing the Estrogen Receptor

Fred Schaufele, Ching-yi Chang, Weiqun Liu, John D. Baxter*, Steven K. Nordeen, Yihong Wan, Richard N. Day, and Donald P. McDonnell

Metabolic Research Unit and Department of Medicine (F.S., W.L., J.D.B.) University of California San Francisco, California 94143

Department of Pharmacology and Cancer Biology (C.-y.C., D.P.M.) Duke University Medical Center Durham, North Carolina 27710

Department of Pathology and Program in Molecular Biology (S.K.N., Y.W.) University of Colorado Health Sciences Center Denver, Colorado 80262

Departments of Medicine and Cell Biology (R.N.D.) National Science Foundation Center for Biological Timing University of Virginia Health Sciences Center Charlottesville, Virginia, 22908

Ligand binding to estrogen receptor (ER) is presumed to regulate the type and timing of ER interactions with different cofactors. Using fluorescence microscopy in living cells, we characterized the recruitment of five different green fluorescent protein (GFP)-labeled ER-interacting peptides to the distinct subnuclear compartment occupied by blue fluorescent protein (BFP)-labeled ERα. Different ligands promoted the recruitment of different peptides. One peptide was recruited in response to estradiol (E_2), tamoxifen, raloxifene, or ICI 182,780 incubation whereas other peptides were recruited specifically by E_2 or tamoxifen. Peptides containing different sequences surrounding the ER-interacting motif LXXLL were recruited with different time courses after E_2 addition. Complex temporal kinetics also were observed for recruitment of the full-length, ER cofactor glucocorticoid receptor-interacting protein 1 (GRIP1); rapid, E_2-dependent recruitment of GRIP1 was blocked by mutation of the GRIP1 LXXLL motifs to LXXAA whereas slower E_2 recruitment persisted for the GRIP1 LXXAA mutant. This suggested the presence of multiple, temporally distinct GRIP 1 recruitment mechanisms. E_2 recruitment of GRIP1 and LXXLL peptides was blocked by coincubation with excess ICI 182,780. In contrast, preformed E_2/ER/GRIP1 and E_2/ER/LXXLL complexes were resistant to subsequent ICI 182,780 addition whereas ICI 182,780 dispersed preformed complexes containing the GRIP1 LXXAA mutant. This suggested that E_2-induced LXXLL binding altered subsequent ligand/ER interactions. Thus, alternative, ligand-selective recruitment and dissociation mechanisms with distinct temporal sequences are available for ERα action *in vivo*. (Molecular Endocrinology 14: 2024–2039, 2000)

0888-8809/00/$3.00/0
Molecular Endocrinology 14(12): 2024–2039

INTRODUCTION

Ligand binding to ER alters ER conformation and thereby affects its interactions with cofactors regulating gene expression (1–3). Many cofactors that interact specifically with the estradiol (E_2)-bound ER or other ligand-bound nuclear receptors contain one or more copies of the consensus sequence LXXLL (4). Mutation of the LXXLL motifs abrogates ligand-dependent cofactor binding to the ligand-binding domain of many nuclear receptors (4, 5). Peptides containing the LXXLL motifs are themselves sufficient to bind to nuclear receptors (6, 7). Structural studies showed that the LXXLL peptides form an amphipathic α-helix, of which the hydrophobic surface fits into a hydrophobic cleft that forms on the surface of the ER ligand-binding domain in response to E_2 binding (6, 7). The ligand-induced hydrophobic cleft is conserved in the ligand

binding domain of most nuclear receptors (8) and is required for ligand-activated transcription via activation function-2 (AF-2) (9).

The hydrophobic cleft does not form properly upon ER binding to tamoxifen or raloxifene (7, 10), which may account for the antiestrogenic action of these ligands in some tissues. Conversely, tamoxifen and raloxifene have estrogenic effects on other tissues. Like estrogens, tamoxifen and raloxifene promote interaction of some cofactors or peptides with ER structures outside of the hydrophobic cleft (11–14). These interactions probably contribute to the AF-2-independent estrogenic actions of tamoxifen and raloxifene. Novel ER ligands that possess estrogenic activities in most tissues and antiestrogenic activities in the breast and uterus will be clinically useful for reducing the estrogen-mediated increase in breast and endometrial tumors that accompanies otherwise beneficial postmenopausal hormone replacement therapies (15–19). Identification of such improved selective estrogen receptor modulators (SERMs) will be aided by the development of techniques that discern the effects of each putative SERM on the types and timing of ER interactions with ligand-selective ER-interacting targets.

Previously we used phage display to isolate a large number of peptides that bound to different sites on nuclear receptors including ERα (12–14). Each peptide differed in their interactions with specific nuclear receptors or in response to different ligands. Some of the nuclear receptor-interacting peptides contained the LXXLL motif and could be grouped into three classes based upon sequence conservation of the two amino acids immediately amino terminal to LXXLL (12). All three classes of LXXLL are naturally found in cofactors that interact with AF-2. Some cofactors contain multiple LXXLL motifs predominantly of a single class. Others contain LXXLL motifs of varying classes and even LXXLL motifs that are distinct from these three classes. It is thought that such divergence in LXXLL sequence (5, 6, 20), combined with nuclear receptor- or ligand-specific divergences in the structure of the hydrophobic activation function-2 cleft (21), and variations in the interactions of cofactors to other nuclear receptor surfaces, contributes to the divergent actions of different ligands and nuclear receptors.

Although the molecular alterations that accompany ligand binding to nuclear receptors have been intensely characterized (1–3), very little is known of the specificity and order of those events within living cells. Recent studies of fluorophore-labeled nuclear receptors and their interacting cofactors (22–27) demonstrated that the temporal and spatial characteristics of nuclear receptors could be directly examined within cells by fluorescence microscopy. Here, we used fluorescence microscopy to measure in intact cells the ligand-specific interactions of ER with the nuclear receptor cofactor GRIP1 and five peptides that we recently selected from combinatorial libraries for their binding to ligand-bound ER (12–14). Human ERα expressed as a fusion with blue fluorescent protein (28) (BFP) localized to discrete subdomains of the nucleus. GRIP1 (glucocorticoid receptor-interacting protein 1) and the peptides expressed in cells as fusions with the spectrally distinct green fluorescent protein (28) (GFP) were more evenly distributed throughout the nucleus; the GFP-peptide fusions were also present in the cytoplasm. When coexpressed with ERα-BFP in cells not treated with ER ligand, the GFP-peptides and GFP-GRIP1 exhibited the same distributions as when expressed alone. When incubated with E_2, three peptides containing variants of LXXLL relocalized to assume the intranuclear position of ER. A fourth, unrelated peptide was selectively recruited in response to tamoxifen whereas recruitment of a fifth peptide was promoted by any of E_2, tamoxifen, raloxifene, or the antiestrogen ICI 182,780. GRIP1 was selectively recruited by E_2 or tamoxifen incubation. Simultaneous incubation with an excess of ICI 182,780 blocked recruitment of GRIP1, each LXXLL peptide, and the tamoxifen-specific peptide.

Recruitment of the peptides and GRIP1 to the intranuclear location of ERα in living cells mimicked their previously reported ligand dependence and efficacy of ERα interaction. In addition to confirming in living cells the ligand specificities of these interactions, the intranuclear recruitment assay uniquely enabled us to determine that each peptide and GRIP1 varied in the timing of recruitment after ligand addition. Surprisingly, temporal studies of dissociation showed that preformed complexes involving LXXLL interactions with ER uniquely were not disrupted even after 4 h of incubation with a 1,000-fold molar excess of ICI 182,780. Thus, we report a novel procedure for investigating the ligand-specific recruitment of labeled factors or peptides to nuclear receptors in living cells. This allowed us to determine the unique timing of different ligand-specific complexes formed with ER and to discover that LXXLL-dependent interactions alter the availability of the receptor for subsequent ligand binding in living cells.

RESULTS

E_2-Dependent Relocalization of Class I, II, and III LXXLL Peptides to the Intranuclear Subcompartment Containing ERα

We previously isolated three different classes of LXXLL-containing, ERα-interacting peptides by phage display (12–14). All three classes are represented in known ERα-interacting cofactors, including a receptor-interacting protein of 140 kDa (RIP140) (29), a thyroid hormone receptor accessory protein of 220 kDa ($TRAP_{220}$) (30), a vitamin D receptor-interacting protein of 205 kDa ($DRIP_{205}$)(31), and the homologous coac-

tivators glucocorticoid receptor-interacting protein (GRIP1) (32, 33), and steroid receptor coactivator (SRC-1a)(34). For instance, RIP140 contains 11 LXXLL motifs, eight of which are of the class III type (S/T,Φ,LXXLL where Φ is any hydrophobic amino acid) whereas $TRAP_{220}$ and $DRIP_{205}$ each contain two LXXLL motifs, both of the class II type (P,Φ,LXXLL). GRIP1 and SRC-1a have, in common, three divergent LXXLL motifs, the most amino terminal of which is of the class I type (S/T, K/R, LXXLL), and two more carboxy-terminal LXXLL motifs that do not readily fit into any of the three classes.

Oligonucleotides encoding peptide sequences representative of each of the class I, II, and III peptides were fused in frame to the carboxy terminus of GFP (see Fig. 1) and expressed in mouse GHFT1–5 cells. The intracellular locations of GFP and each GFP-labeled LXXLL peptide were identified by fluorescence microscopy after their expression. GFP (not shown) and the three GFP-LXXLL fusions were distributed throughout the cytoplasm and nucleus (Fig. 2, A–C, *left panels*). The proportion of GFP-LXXLL fluorescence in the nucleus and cytoplasm varied from evenly distributed between nucleus and cytoplasm to some nuclear preference. The variation in nuclear/cytoplasmic partitioning was independent of expression level and was globally similar for GFP and each GFP-LXXLL fusion.

To determine whether ERα expression altered the distribution of GFP-LXXLL, ERα was coexpressed as an in-frame fusion with BFP. This allowed us to separately track the locations of ERα-BFP and GFP-LXXLL in the same cell by selectively exciting and detecting their corresponding blue and green emissions (35). The ERα-BFP fusion was functional as, like native ERα (36), it cooperated with the transcription factor Pit-1 to activate the PRL promoter in GHFT1–5 cells (not shown). The ERα-BFP fusion also activated the transcription of a minimal promoter under the control of an isolated ER binding site in HeLa and DU145 cells (not shown). In contrast to the cytoplasmic and uniform intranuclear distributions of GFP-LXXLL, ERα-BFP was exclusively nuclear and assumed a reticular pattern of distribution within the nucleus (Fig. 2, ERα-BFP). This reticular intranuclear distribution has been previously reported for ER (22, 27) as well as other nuclear receptors (23–26) and is more pronounced

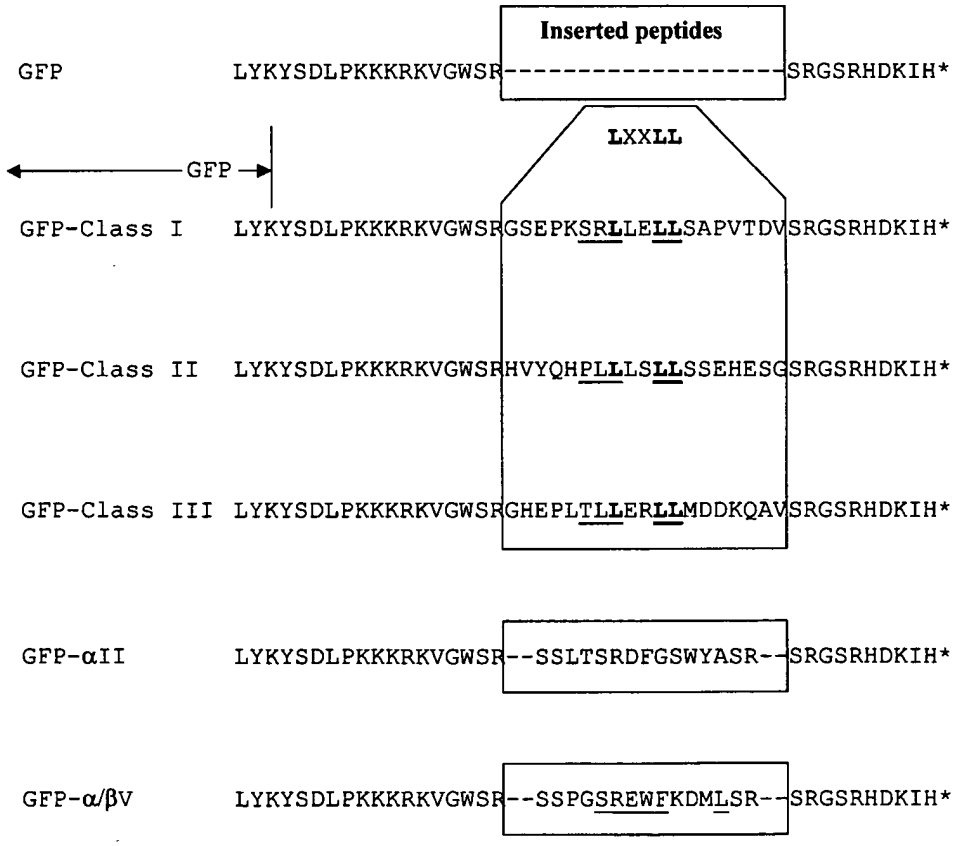

Fig. 1. ER-Interacting Peptides Fused to the Carboxy Terminus of GFP

Box represents sequence of ER-interacting peptides isolated in Chang *et al.* (12) and Norris *et al.* (13). *Underlined* amino acids in peptide sequence are those conserved in the class I, class II, and class III LXXLL peptides (12). *Underlined* in the α/βV peptide are those amino acids conserved in other isolated peptides and in receptor potentiating factor 1 (13). *, Carboxy terminus of fusion proteins. The spacer between GFP and the ER-interacting peptide sequence contains the Simian Virus 40 NLS that, because of the small size of GFP, did not have much effect on nuclear localization.

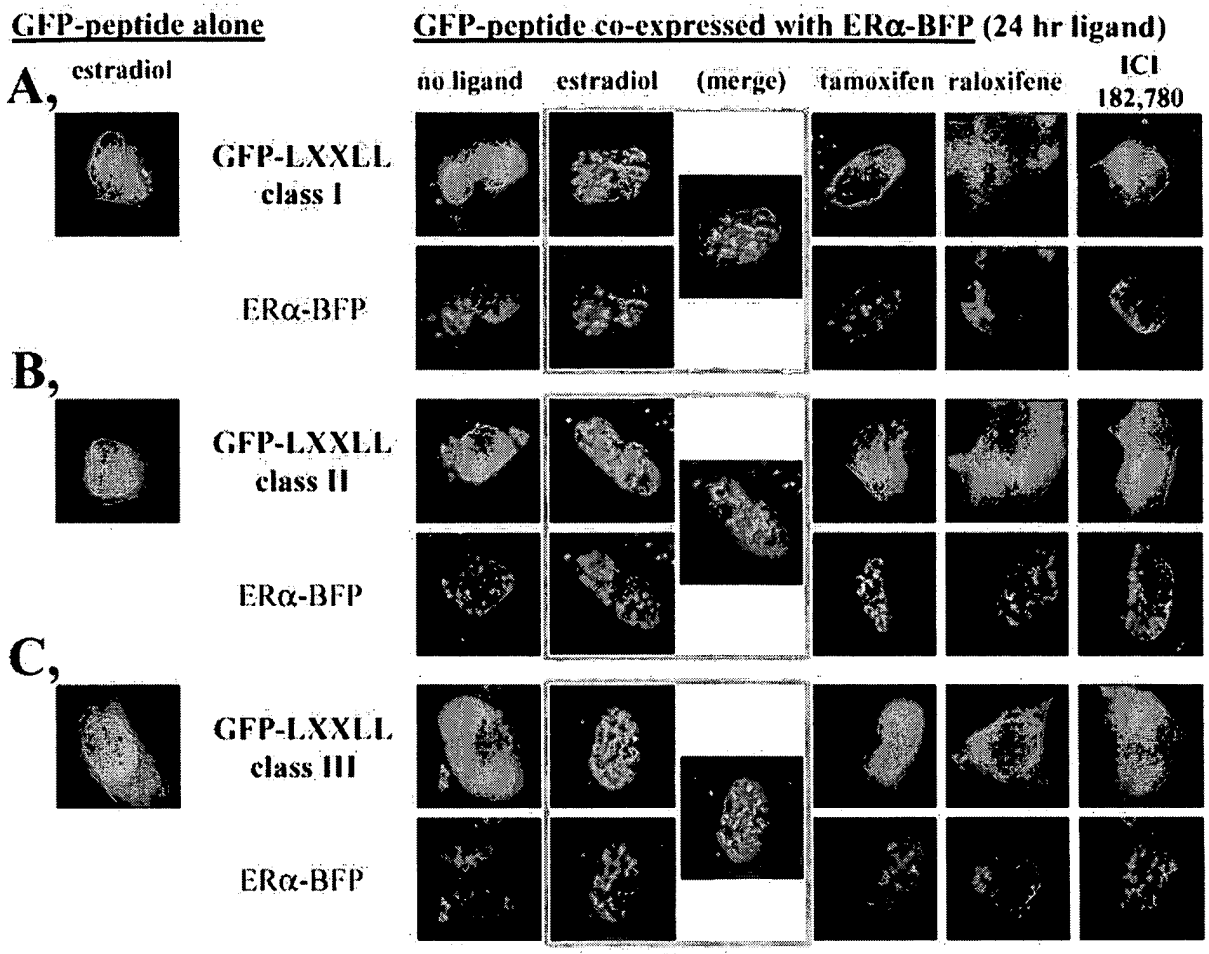

Fig. 2. E_2-Dependent Recruitment of GFP Fused to Class I, Class II, and Class III LXXLL Peptides to the Intranuclear Location of ERα-BFP

Fluorescence microscopic detection of the intracellular localization of the three GFP-LXXLL fusions (A–C) coexpressed with ERα-BFP in cells. One day after transfection, cells were treated either with ethanol vehicle (no ligand), 10^{-8} M estradiol, 10^{-6} M tamoxifen, 10^{-7} M raloxifene or 10^{-7} M ICI 182,780. One day after ligand addition, green and blue fluorescence was selectively detected by fluorescence microscopy as described in *Materials and Methods*. *Merge*, Merged blue and green images of the cells incubated with E_2 indicate overlap in the intranuclear location of ERα-BFP and each GFP peptide as a cyan coloration. Green fluorescence from each GFP-peptide fusion in the absence of ERα-BFP expression is shown from cells incubated with 10^{-8} M estradiol (*left panels*).

when the cells are incubated with E_2 or SERMs (22, 27).

In cells grown in E_2-free media, the dispersed cellular distribution of each GFP-LXXLL fusion was unchanged upon coexpression of ERα-BFP (Fig. 2, A–C, no ligand). In contrast, incubation of cells coexpressing ERα-BFP and any of the GFP-LXXLL fusions with 10^{-8} M E_2 caused the GFP-LXXLL to assume the reticular pattern characteristic of ERα-BFP in the nucleus (Fig. 2, A–C, estradiol). Complete overlap of GFP-LXXLL with ERα-BFP in the identical subnuclear compartment after E_2 addition is indicated by the exclusively cyan-colored image obtained when the separate blue and green images are merged (Fig. 2, A–C, merge). This was observed in cells that express GFP-LXXLL in low stoichiometry relative to ERα-BFP. In cells expressing more GFP-LXXLL than ERα-BFP, colocalization of GFP-LXXLL and ERα-BFP was observed as a concentration of green fluorescence at the site of blue fluorescence (not shown). When ERα-BFP was not coexpressed, there was no intranuclear redistribution of GFP-LXXLL in the presence of E_2 (Fig. 2, A–C, *left panels*) or any other ER ligand (not shown). Similarly, GFP itself did not redistribute to ERα-BFP upon incubation with E_2 or any other ER ligand (not shown). Thus, relocalization of GFP-LXXLL was specifically dependent upon the LXXLL peptide, coexpression of ERα-BFP, and addition of E_2.

Intracellular Relocalization of Different LXXLLs to ERα Parallels Their Interaction Profiles

To further characterize the ligand dependence of GFP-LXXLL colocalization with ERα-BFP, we determined

the E_2-induced relocalization kinetics of each of the class I, class II, and class III GFP-LXXLLs to ERα. Each GFP-LXXLL was coexpressed with ERα-BFP in cells grown in E_2-free media. One day after transfection, parallel coverslips were incubated with no hormone, or with 10^{-10}, 10^{-9}, 10^{-8} or 10^{-7} M E_2 for 24 h. We then determined the fraction of cells in which GFP-LXXLL colocalized with ERα-BFP for each E_2 concentration.

By fluorescence microscopy, we scanned the coverglass using blue fluorescence excitation and emission filters to first identify cells expressing ERα-BFP. We then rapidly switched to the green filter set to determine whether the cell contained visible GFP-linked target. If the GFP-linked target was also present, it was then scored as colocalized if there was any concentration of green fluorescence at the site of the ER. By scoring GFP-peptide or cofactor-expressing cells only after determining which cells obviously contained ERα-BFP, we avoided the bias in which a bright, reticular GFP fluorescence pattern would inflate our detection of colocalized cells containing otherwise undetectable levels of the generally less fluorescent ERα-BFP. By setting the colocalization criterion as "any" colocalization, we also removed any biases that would have resulted if we had attempted to subjectively score cells for the variable extent of colocalization. Since the proportion of non-colocalized cells decreases with increasing colocalization, the recruitment of specific factors or peptides is measured as the change in the proportion of cells that responded after the addition of different concentrations of E_2. The validity of this approach was confirmed by the high reproducibility of the data obtained from multiple independent experiments, which are plotted in Fig. 3A as the mean ± SD in the percent of cells showing colocalization at each ligand concentration. Half-maximal binding to ERα-BFP with each class of GFP-LXXLL was reached at 3–7 × 10^{-10} M E_2, approximately the concentration of E_2 needed for activation of ER-regulated promoters in cell transfection studies (37).

Essentially complete colocalization with ERα-BFP was achieved with 10^{-8} M E_2 for both the class I and the class III GFP-LXXLL fusions. In contrast, colocalization of the class II GFP-LXXLL did not increase beyond a maximum of 57 ± 6% of the cells. This limit did not appear to be a function of the level of peptide expressed in the cell as the proportion of cells showing colocalization remained constant over a wide range of GFP-class II LXXLL expression (Fig. 3B). In these studies, expression of GFP-LXXLL was modulated from a tetracycline-inducible promoter by varying the levels of the inducer, doxycycline. Note that all images in Fig. 3B were taken with the same short exposure times that were insufficient to detect the basal expression level of the GFP-LXXLL peptide in the absence of doxycycline. Thus, the observed deficiency in the *in vivo* ERα-BFP interaction of the class II LXXLL relative to the class I and III LXXLLs was not related to differences in the expression of these peptides. The reduced efficiency of colocalization of the GFP-class II LXXLL with ERα-BFP accurately mimicked the poorer interaction of the class II peptide with ERα that we had previously observed (12).

Delayed Temporal Kinetics of Class II LXXLL Recruitment to ERα

Sequence-specific differences in colocalization of the three LXXLL peptides with ERα were also evident in time course studies. We conducted single cell recordings of the E_2-induced intracellular recruitment of LXXLL to ERα. First, we identified cells, grown in the absence of E_2, that expressed both the class I GFP-LXXLL and ERα fused to red fluorescent protein (RFP). The ERα-RFP fusion protein was functionally active in the ligand-induced activation of estrogen-responsive promoters (data not shown). ERα-RFP and GFP-LXXLL digital images of the same cell were captured using red and green fluorescent filter sets before the addition of ligand and at 1-min intervals after the addition of 10^{-6} M E_2. An example of one cell before E_2 addition and 20 min after E_2 addition is provided in Fig. 4A. Appropriate controls, using cells expressing only ERα-RFP or GFP-LXXLL of intensities equivalent to those in the coexpressing cells, showed that there was no fluorescence bleedthrough between the red and green images (not shown).

Only partial colocalization of GFP-LXXLL with ERα-RFP (or ERα-BFP) was obtained after these short incubation periods (see Fig. 4A), which contrasts with the complete overlap of GFP-LXXLL and ERα-RFP (or ERα-BFP) after 24-h incubations (Fig. 2). To quantify partial colocalization at the short time frames, we measured the intensity of green GFP-LXXLL and red ERα-RFP fluorescence for each pixel within the nucleus of each cell image. The intensity of green fluorescence within the nucleus that colocalized with the red fluorescence of ERα-RFP was divided by the intensity of green fluorescence in the regions of the nucleus from which ERα-RFP was less concentrated (defined at those regions of the nucleus in which ERα-RFP intensity was less than 75% of the maximal ERα-RFP intensity). This ratio was calculated before the addition of hormone and at 1-min time intervals after E_2 addition for 15 different single cell recordings. The change in this ratio is plotted over 20 min after E_2 addition in Fig. 4B; a positive change in the pixel intensity ratio indicates that more GFP-LXXLL was concentrating at the intranuclear location of ERα-RFP. Notably, the response for each cell varied from cells displaying relatively random fluctuations of green/red pixel intensities of −0.02 to +0.02 to cells in which there was an obvious concentration of the GFP-LXXLL at the intranuclear location of ERα-RFP over the 20-min time course. For comparison, the read-out obtained from a cell shown in Fig. 4A, in which con-

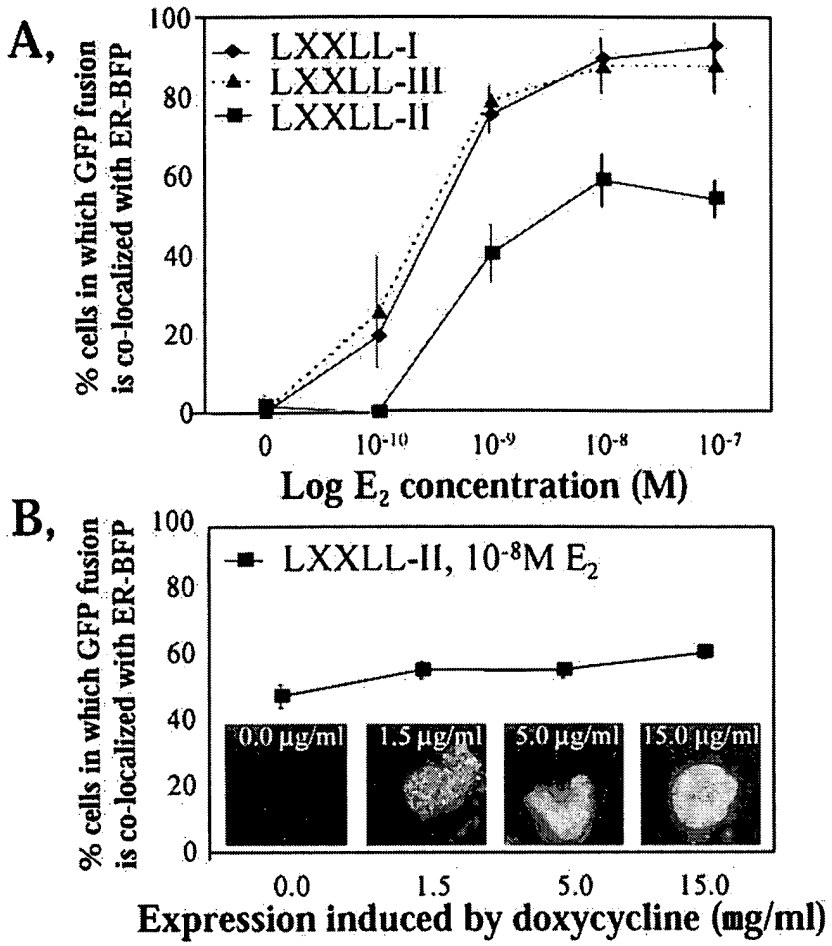

Fig. 3. Different LXXLL-Containing Peptides Are Recruited to ERα with Different Kinetics

A, The proportion of cells in which class I, class II, or class III GFP-LXXLL colocalizes with ERα-BFP increases with increasing E_2 dose. Half-maximal colocalization is achieved at E_2 concentrations required for promoter activation (37, 50). The *graph* represents the mean ± SD in the percent of cells displaying colocalization from three independent experiments. B, The poorer colocalization of the class II GFP-LXXLL with ERα-BFP is independent of the expression level of class II GFP-LXXLL. Representative green fluorescence from individual cells shows the different expression levels of class II GFP-LXXLL induced by the indicated concentrations of doxycycline used to drive the linked tetracycline-inducible promoter. In the absence of doxycycline, green fluorescence was visible but not captured with the short exposure times used to collect the images shown. The *graph* represents the mean ± SD in the percent of cells displaying colocalization from a single transfection collected three separate times over 1 day.

centration of GFP-LXXLL at the site of ERα-RFP is at the threshold of being visible by the naked eye, is indicated by the *open triangles* (see Fig. 4B, *). Thus, over short time periods, recruitment of GFP-LXXLL to ERα-RFP, measured quantitatively, is highly variable with time after E_2 addition.

The cell-to-cell variability in recruitment over short time periods required that we score large numbers of cells at each time point to obtain data in which we have confidence. This could not be accomplished by recording individual cells for prolonged time periods. However, our prior experience demonstrated that we could readily and reproducibly score by visual inspection 50–150 cells within a 10-min window (Fig. 3). We coexpressed each GFP-LXXLL together with ERα-BFP in cells grown in the absence of ligand and then scored those cells, exactly as for Fig. 3, for colocalization in 10-min windows between 15–25 min, 40–50 min, and 85–95 min at 24 h after the addition of 10^{-8} M E_2 (Fig. 4C).

Colocalization of the class I and class III GFP-LXXLLs with ERα-BFP was detected within 20 min after the addition of 10^{-8} M E_2 and increased thereafter. This represented the time required for E_2 to enter the cell, bind to ERα-BFP, and have detectable amounts of freely diffusing GFP-LXXLL concentrate at the intranuclear location of the liganded ERα-BFP. Whereas the colocalization of GFP-class I LXXLL and GFP-class III LXXLL fusions with ERα-BFP showed identical time courses and reached similar levels in response to saturating levels of E_2, the redistribution of the class II peptide to ERα-BFP was much less rapid (Fig. 4C).

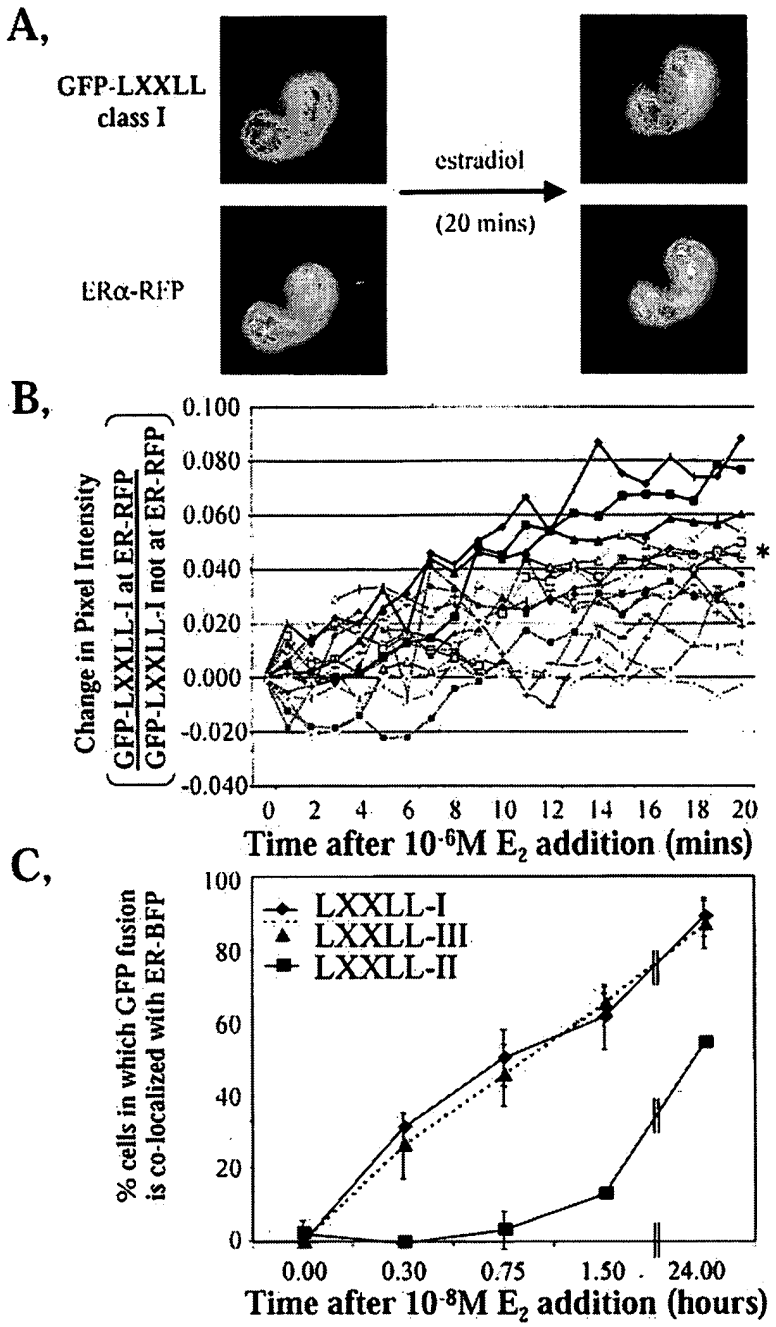

Fig. 4. Different LXXLL-Containing Peptides Are Recruited to ERα with Different Temporal Kinetics

A, Sequential images of the same cell captured before and 20 min after the addition of 10^{-6} M E_2 demonstrate partial colocalization of the class I LXXLL-GFP fusion protein with ERα fused to RFP. B, Quantification of the level of GFP and RFP fluorescence at each pixel within the nucleus at 1-min time intervals after the addition of 10^{-6} M E_2 shows variable concentration of class I LXXLL-GFP at the position of ERα-RFP in 15 different cells. *, Readout of cell shown in Fig. 4A (*open triangles*). C, The proportion of cells showing any colocalization of ERα-BFP with each GFP-LXXLL was scored with time after addition of 10^{-8} M E_2. The slower time course and reduced binding of the class II peptide reflect the previously reported poorer interaction of this peptide with ERα (12). Each *graph* represents the mean ± SD deviation in the percent of cells displaying colocalization from three independent experiments.

The delayed time course of class II LXXLL intracellular colocalization with ERα-BFP, which would not have been detected in other assays, demonstrated that ER association with different LXXLL sequences follows different temporal kinetics. An intriguing possibility is that the different LXXLL temporal kinetics underlies a previously proposed (38) sequential recruitment of co-factors to ER after E_2 addition.

Table 1. Ligand-Specific Complexes Formed by ERα and Indicated Peptides or GRIP1

Ligand : (24 hour incubation) / GFP -	no ligand	ICI 182,780 5×10^{-7}M	Raloxifene 5×10^{-7}M	Tamoxifen 5×10^{-7}M	Estradiol 5×10^{-8}M	ICI inhibition: E_2, 10^{-9}M or Tam, 10^{-7}M → to αβV	+ ICI, 10^{-6}M
LXXLL -I	2 +/- 2%	0 +/- 0%	0 +/- 0%	21 +/- 9%	93 +/- 6%	79 +/- 7%	0 +/- 0%
LXXLL -II	2 +/- 2%	1 +/- 1%	1 +/- 1%	3 +/- 2%	64 +/- 17%	47 +/- 4%	0 +/- 0%
LXXLL -III	0 +/- 0%	*	*	*	90 +/- 8%	76 +/- 4%	3 +/- 1%
αII	0 +/- 0%	85 +/- 8%	46 +/- 5%	76 +/- 1%	56 +/- 2%	32 +/- 11%	84
α/βV	0 +/- 0%	0 +/- 0%	2 +/- 2%	81 +/- 14%	2 +/- 2%	52 +/- 10%	1 +/- 0%
GRIP1 wt	9 +/- 5%	3 +/- 3%	4 +/- 3%	21 +/- 12%	81 +/- 17%	63 +/- 17%	6 +/- 3%
GRIP1 ΔLXXLL	6 +/- 3%	3 +/- 3%	0 +/- 0%	5 +/- 4%	48 +/- 6%	43 +/- 5%	3 +/- 1%

*, no co-localization in some LXXLL-III data not quantified by cell counting

shading represents indicated % co-localization with ERα

X% 0-9% | X% 10-34% | X% 35-59% | X% 60-89% | X% 90-100%

Ligand-Specific Differences in Class I, II, and III LXXLL Colocalization with ERα

Incubation of cells coexpressing GFP-LXXLL and ERα-BFP overnight with 10^{-6} M tamoxifen resulted in a slight concentration of green fluorescence emitted from the class I GFP-LXXLL over the reticular pattern of ERα-BFP fluorescence (Fig. 2A). This weak colocalization was reproducible and was quantified in Table 1 as the percentage of cells in which the indicated GFP-linked peptide showed any visible colocalization with ERα-BFP in response to the indicated ER ligand. Tamoxifen promoted class I GFP-LXXLL colocalization with ERα-BFP but not class III GFP-LXXLL colocalization with ERα-BFP (Table 1). Thus, the class I and class III peptides, which behaved identically in response to E_2 (Figs. 3A and 4C), differed in their response to tamoxifen. The class II GFP-LXXLL also did not appreciably respond to tamoxifen (Table 1).

In contrast to tamoxifen, incubating the cells overnight with two other SERMs, raloxifene or ICI 182,780, did not promote overlap in the intracellular distributions of coexpressed ERα-BFP and any of the class I, II, or III GFP-LXXLLs (Table 1). Raloxifene and ICI 182,780 were effective in promoting the colocalization of another, unrelated peptide with ERα-BFP (Fig. 5A). This peptide, αII, was previously selected for the ability to interact with ERα bound by either E_2 or tamoxifen (13). In the absence of ligand, the intracellular distribution of GFP-αII was diffuse (Fig. 5A). However, E_2, tamoxifen, raloxifene, and ICI 182,780 each induced GFP-αII to redistribute to the intranuclear location occupied by ERα-BFP (Fig. 5A and Table 1). Relocalization was specifically dependent upon the αII peptide, ERα-BFP coexpression, and ligand addition. Thus, E_2, tamoxifen, raloxifene, and ICI 182,780 were all capable of entering the cell and promoting specific ERα-peptide interactions. The different ligand specificities of

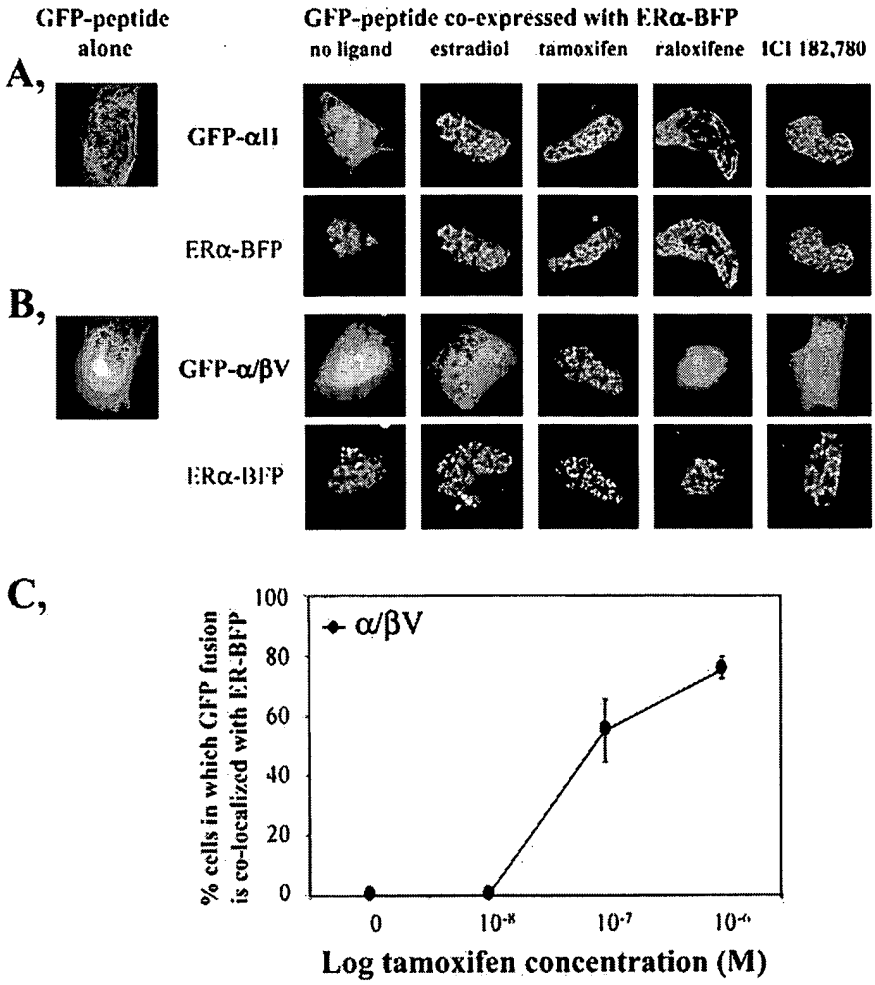

Fig. 5. Different Ligand Dependence of the Recruitment of non-LXXLL-Containing, ER-Interacting Peptides to the Intranuclear Location of ERα

A, Intracellular recruitment of GFP fused to the αII peptide (13) to ERα-BFP is induced by incubating the cells with any of E_2, tamoxifen, raloxifene, or ICI 182,780. B, Tamoxifen-dependent, intranuclear colocalization of ERα-BFP and GFP fused to the α/βV peptide (13). Ligand incubation and fluorescence detection are as described in the legend to Fig. 2. Green fluorescence from each GFP-peptide fusion in the absence of ERα-BFP expression (*left panels*) is shown from cells incubated with 10^{-8} M E_2 (A) or 10^{-6} M tamoxifen (B). C, Half-maximal recruitment of GFP-α/βV to ERα-BFP is achieved at tamoxifen concentrations that parallel tamoxifen induction of ERα promoter activation (13). The *graph* represents the mean ± SD in the percent of cells displaying colocalization from three independent experiments.

the LXXLL and αII peptide interactions demonstrate the subtle differences in receptor conformation promoted by each ligand.

Tamoxifen-Specific Colocalization of an ER-Interacting Peptide with ERα-BFP

SERM-selective *in vivo* recruitment also was shown by the tamoxifen-specific recruitment of another peptide, α/βV, selected previously from a combinatorial library for interaction only with ERα bound to tamoxifen (13). We fused the α/βV peptide in frame to GFP (Fig. 1) and determined that, like GFP, GFP-LXXLL, and GFP-αII, the GFP-α/βV fusion distributed throughout the nucleus and was present to varying degrees in the cytoplasm (Fig. 5B). In cells not expressing ERα-BFP, GFP-α/βV remained distributed after treatment with tamoxifen (Fig. 5B, *left panel*) or any other ligand. Similarly, when coexpressed with ERα-BFP in cells grown in the absence of ligand or after incubation with 10^{-8} M E_2, 10^{-7} M raloxifene, or 10^{-7} M ICI 182,780, the subcellular localization of GFP-α/βV was not altered. In contrast, incubation with 10^{-6} M tamoxifen resulted in a concentration of GFP-α/βV at the intranuclear reticular pattern characteristic of ERα-BFP. Tamoxifen dose-response curves (Fig. 5C) showed that GFP-α/βV relocalization to ERα-BFP corresponded with the promoter activation profile of tamoxifen bound to ERα (37). Tamoxifen-selective GFP-α/βV colocalization with ERα-BFP demonstrated that ERα

adopts a conformation *in vivo* that is different than that adopted by the E_2-, raloxifene-, or ICI 182,780-bound receptors.

Ligand-Dependent Recruitment of the Full-Length ER-Interacting Cofactor GRIP1 to the Intranuclear Compartment Containing ERα

The ligand-specific and temporally distinct associations of different ER-interacting peptides with ERα suggested that a similar approach could be employed to demonstrate the ligand specificity and pattern of recruitment of full-length ER-interacting cofactors to ERα *in vivo*. Indeed, one ER coactivator SRC-1a fused to GFP recently was shown to be recruited to the intranuclear location of ERα fused to the cyan fluorescent protein upon E_2, but not tamoxifen or ICI 182,780, incubation (27). We determined that the related ER-interacting cofactor GRIP1, fused to GFP, was also recruited upon ligand addition to the intracellular subcompartment containing ERα-BFP (Fig. 6) and then detailed the ligand specificity and kinetics of that recruitment (Fig. 7).

GFP-GRIP1, when expressed by itself, was exclusively nuclear and dispersed throughout the intranuclear compartment, although absent from nucleoli (Fig. 6A). In cells coexpressing GFP-GRIP1 and ERα-BFP and incubated with ICI 182,780 or raloxifene, GFP-GRIP1 retained its characteristic dispersed distribution (Fig. 6B). In contrast, both E_2 and tamoxifen were very effective in recruiting GFP-GRIP1 to ERα-BFP (Fig. 6B and Table 1). This again illustrated that E_2 and each SERM promote very distinct ER interactions with specific ER-interacting factors and motifs.

Temporal Variation in LXXLL Requirements for E_2 and Tamoxifen Recruitment of GRIP1 to ERα

E_2 and tamoxifen-specific recruitment of GFP-GRIP1 to ERα-BFP was distinguished by their different time courses and dependencies upon the LXXLL motifs in GRIP1 (Fig. 7). E_2 recruitment was characterized by a rapid LXXLL-dependent phase followed by a slow LXXLL-independent phase. Rapid recruitment was detected as an initial plateau of 30–40% of the cells displaying colocalization of GFP-GRIP1 with ERα-BFP within 20 min after E_2 addition (Fig. 7A, GRIP1-wt). This early phase plateau was blocked (Fig. 7A, GRIP1-ΔLXXLL) by mutation to LXXAA of the two LXXLL motifs of GRIP1 required for interaction with the ER

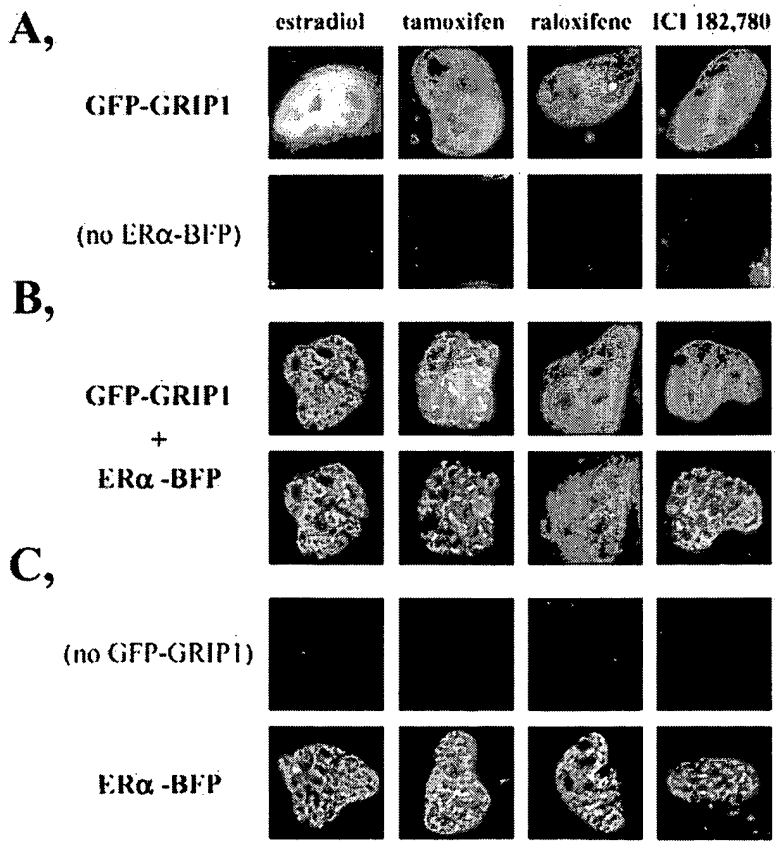

Fig. 6. Recruitment of GRIP1 to the Intranuclear Location of ERα Is Ligand-Selective

A, In the absence of coexpressed ERα-BFP, GRIP1 is evenly distributed throughout the nucleoplasm but is absent from nucleoli. B, When coexpressed with ERα-BFP, GFP-GRIP1 assumes the intranuclear location of ERα-BFP only if incubated with E_2 or tamoxifen. C, Cells expressing ERα-BFP only. Ligand incubation and fluorescence detection are as described in the legend to Fig. 2.

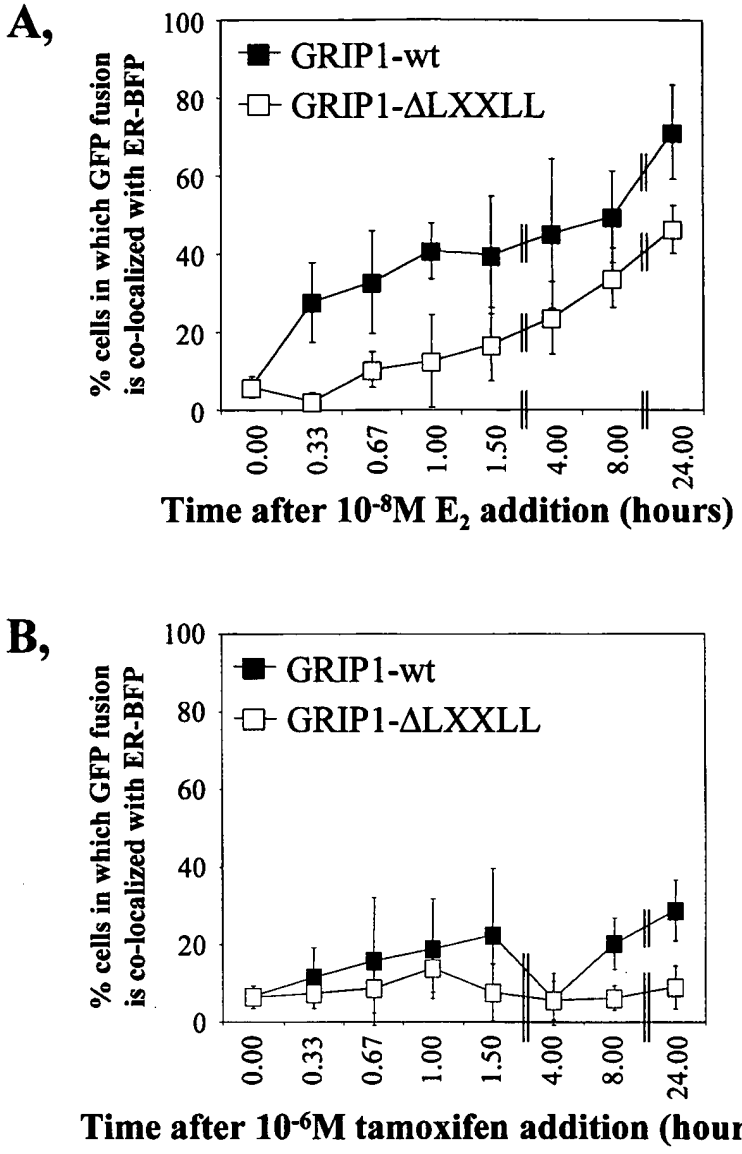

Fig. 7. Different Temporal Kinetics for LXXLL-Dependent and LXXLL-Independent Recruitment of GFP-GRIP to ERα-BFP

A, The proportion of cells in which GRIP1 colocalizes with ERα-BFP increases rapidly with time after E_2 addition. Rapid colocalization is lost if the second and third LXXLL motifs of GRIP1 are mutated to LXXAA (GRIP1-ΔLXXLL). GRIP1-ΔLXXLL is still induced by E_2 to colocalize with ERα but with much reduced temporal kinetics indicating that two separate, and temporally distinct mechanisms govern E_2-dependent, intranuclear recruitment of GRIP1 to ERα. B, Recruitment of GRIP1 to the intranuclear location of ERα is LXXLL-dependent at 8 h or more after tamoxifen addition. Recruitment at earlier time points is variable, but not statistically significant. Each *graph* represents the mean ± SD in the percent of cells displaying colocalization from three independent experiments.

ligand binding domain (5). A more gradual increase in GRIP1/ERα colocalization that followed 1.5 h after E_2 addition was not abrogated by the LXXAA mutations. These complex temporal kinetics and LXXLL dependencies suggest time-dependent variations in the available types of E_2/ER/GRIP1 associations with some lagging associations possibly dependent upon interim interactions and/or enzymatic processes.

The weaker tamoxifen-dependent recruitment of GFP-GRIP1 to ERα-BFP also displayed a complex time course (Fig. 7B) that was mechanistically distinct from that induced by E_2. Tamoxifen-induced colocalization of GFP-GRIP1 and ERα-BFP was statistically significant at 8 and 24 h after tamoxifen addition. Before that, a slow gradual recruitment of GRIP1 was not statistically significant. A precipitous drop in colocalization at 4 h after tamoxifen addition may indicate some tendency toward a temporally biphasic response, but this interpretation is questionable given that the change in colocalization at the early time points was not statistically significant. The statistically significant tamoxifen-dependent colocalization at 8

and 24 h was disrupted by the mutation of the GRIP1 LXXLL motifs to LXXAA (Fig. 7B). Because it is unlikely that the LXXLL motifs of GRIP1 interact directly with the tamoxifen-bound ER, the LXXLL dependence of the slow, tamoxifen-dependent GRIP1 recruitment may reflect a more indirect recruitment of GRIP1 to the tamoxifen-bound ER or a dependence on additional motifs present in GRIP1.

E_2/ERα/LXXLL Complexes Become Resistant to Subsequent Challenge with Antiestrogen

Previous reports showed that ligand-induced binding of LXXLL to ER *in vitro* caused an alteration in the rate by which the ligand dissociates from the ER (39). To determine whether LXXLL interaction with ER *in vivo* might similarly slow ligand access to ER, we examined whether ERα/cofactor or ERα/peptide complex formation altered access to the antiestrogen ICI 182,780. ICI 182,780 did not promote ERα-BFP colocalization with GFP-GRIP1, GFP-α/βV, or any of the three GFP-LXXLL fusions (Table 1). Consistent with its role as an antiestrogen, simultaneous addition of 10^{-6} M ICI 182,780 with 10^{-9} M E_2 abrogated colocalization of ERα-BFP with each of the three GFP-LXXLL fusions and GFP-GRIP1 (Table 1, ICI inhibition) whereas colocalization of the ICI 182,780-responsive, αII peptide was unaffected. ICI 182,780 (10^{-6} M) also blocked colocalization of ERα-BFP and GFP-α/βV in response to 10^{-7} M tamoxifen (Table 1).

Having showed that 10^{-6} M ICI 182,780 effectively blocked recruitment of GRIP1 and the α/βV, LXXLL-I, LXXLL-II and LXXLL-III peptides to ERα, we next determined the temporal kinetics of complex dissociation. To do so, we challenged preformed complexes with an excess of ICI 182,780 to block the reformation of transiently dissociated complexes. Initially, the proportion of cells containing ERα colocalized with GFP-α/βV after 24 h incubation with 10^{-7} M tamoxifen was determined, 10^{-6} M ICI 182,780 was added to the media, and the cells subsequently were scored for any colocalization at the indicated time points after ICI 182,780 addition (Fig. 8A). Complete disruption of colocalization of GFP-α/βV and ERα-BFP was observed within 2 h of ICI 182,780 addition. This established that 2 h was sufficient time for ICI 182,780 to enter the cells, disrupt all preformed complexes, and completely release all GFP-α/βV concentrated at the ERα subcompartment.

For complexes of ERα with GRIP1, the GRIP1 LXXAA mutant, and the LXXLL peptides, dissociation by 10^{-6} M ICI 182,780 was assessed after a 24-h treatment with 10^{-9} M E_2. In contrast to the α/βV peptide, GRIP1 remained as tightly associated with ERα 4 h after ICI 182,780 addition as it was before ICI 182,780 addition (Fig. 8B). Complete resistance to ICI 182,780 challenge also was observed for E_2/ER/GRIP1 complexes formed after only 1 h of E_2 preincubation (not shown). The relative stability of the E_2/ER/GRIP1 complexes depended upon the integrity of the LXXLL sites as GRIP1 containing the LXXAA mutations was dispersed by ICI 182,780 addition in a time-dependent fashion (Fig. 8B). The E_2/ER/GRIP1 complexes similarly displayed an LXXLL-dependent resistance to challenge with 10^{-6} M raloxifene (not shown). These data suggested that interaction of the LXXLL motif with ERα might regulate the subsequent ligand access to ERα *in vivo* as suggested by *in vitro* studies (39). Indeed, ERα complexes formed with the isolated LXXLL peptides were also resistant to dispersal by ICI 182,780 (Fig. 8C), demonstrating that interaction with LXXLL alone was sufficient to alter the subsequent response of the preformed complexes to challenge with ligand.

DISCUSSION

We found that different ER ligands caused the recruitment of specific panels of nuclear receptor-interacting peptides and proteins to the intranuclear location occupied by ERα (Figs. 2, 5, and 6). The correlation of the ligand specificities of intranuclear recruitment (Figs. 2–7 and Table 1) with the previously reported ligand specificities of the direct interactions of GRIP1 and each peptide with ERα (6, 7, 12–14, 20) suggests that some colocalization involves direct interactions between ERα-BFP and the GFP-linked GRIP1 and target peptides. Consistent with direct interaction, simultaneous addition of an excess of antiestrogen also blocked intranuclear recruitment. Thus, recruitment in living cells faithfully reflected the known biochemical and molecular properties of well characterized ER-interacting factors.

In addition to confirming in living cells the ligand specificities of these previously known interactions, the analysis of intranuclear recruitment allowed us to follow complex formation with time after ligand addition. Temporal variations in both recruitment and dissociation were observed (Figs. 4, 5, 7, and 8). Temporally delayed recruitments may represent a secondary association of some complexes via intermediary factors that are initially recruited in response to ligand binding. Such an indirect interaction may be responsible for the delayed (Fig. 7) interaction of ERα with GRIP deleted of the two LXXLL motifs previously described (5) to be necessary for direct GRIP1 interaction with ERα. Alternatively, GRIP1 is known to interact with other regions of ERα (11), and the temporal delay of intranuclear recruitment of GRIP1ΔLXXLL may result from time-dependent ERα interactions or modifications that may be required for the proper folding of these alternative GRIP1 interaction sites.

The molecular basis for the delayed recruitment to ERα of the isolated class II LXXLL (Fig. 4C) similarly remains to be defined. However, the direct interaction of the class II peptide with AF-2 in ERα is weak compared with the class I and class III LXXLL interactions (12), and the delayed intracellular recruitment may

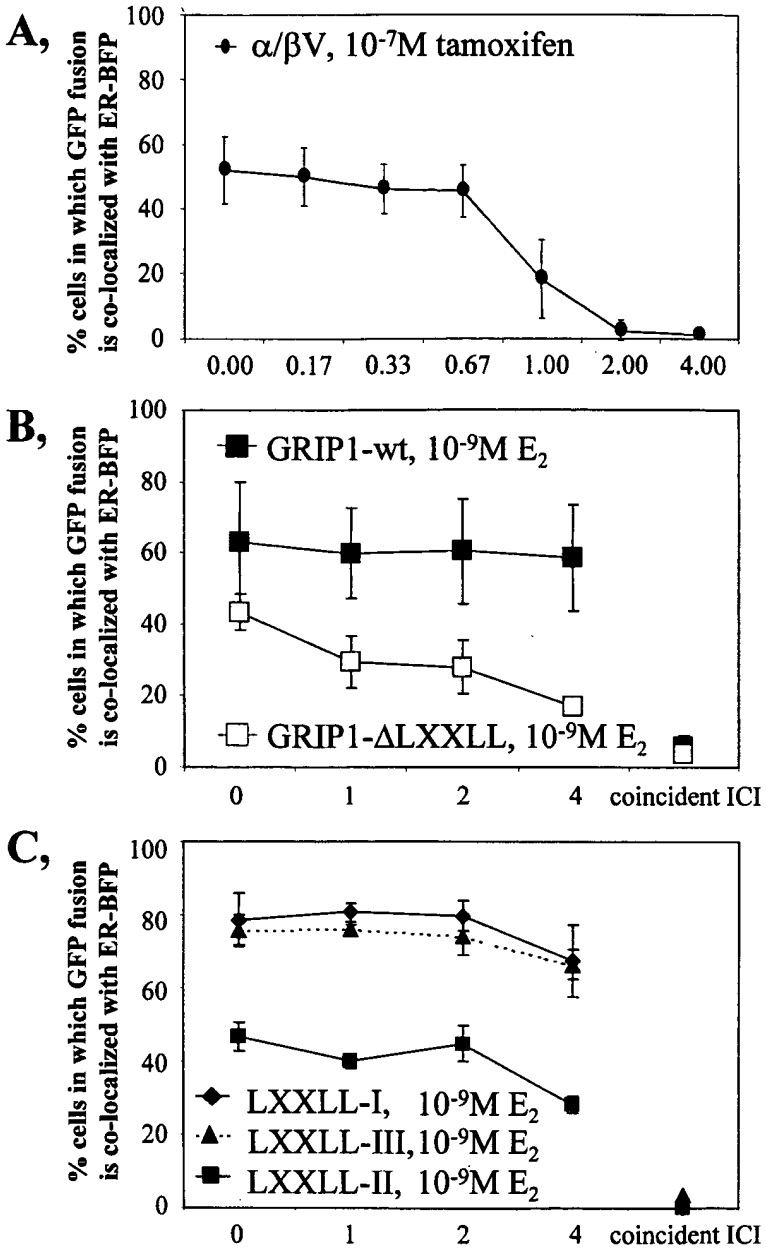

Fig. 8. Colocalized E_2/ERα/LXXLL Complexes Are Resistant to Dispersal by Antiestrogen

A, Colocalization of the non-LXXLL-containing GFP-α/βV peptide with ERα-BFP induced by 10^{-7} M tamoxifen is reversed by subsequent incubation with 10^{-6} M ICI 182,780. Complexes of ERα with GRIP1 (panel B) and each of the LXXLL peptides (panel C) induced by 10^{-9} M E_2 are not disrupted even 4 h after the addition of 10^{-6} M ICI 182,780. In contrast, colocalized GRIP1-ΔLXXLL is readily dispersed from the intranuclear location of ERα upon ICI 182,780 addition. Coincident ICI, percent cells showing colocalization 24 h after simultaneous addition of 10^{-6} M ICI 182,780 and 10^{-9} M E_2 in parallel experiments. Each *graph* represents the mean ± SD in the percent of cells displaying colocalization from four independent experiments.

arise from class II LXXLL E_2-induced associations with other regions of ERα, other ER-interacting factors, or even with ERα covalently modified by cofactors recruited to the E_2-bound ER. Although the mechanisms for these temporal variations in intranuclear recruitment remain unknown, the previously unrecognized variations in the timing and sequence of complexes recruited to ER after ligand addition are likely to be a key determinant of ligand response and adaptation and are uniquely detected by the intranuclear recruitment assay.

Challenge of the preformed complexes with competitive antagonists demonstrated that each peptide or cofactor was displaced from the complexes with

unique dissociation kinetics (Fig. 8). Complexes of ERα with LXXLL-containing peptides or cofactors were considerably more resistant to disruption by ICI 182,780 or raloxifene than complexes that did not involve LXXLL interactions, demonstrating that specific ligand-dependent interactions uniquely changed the nature of the complexes. The LXXLL-dependent reduction in the dissociation kinetics of the preformed complexes may be a consequence of the decreased off rate of ligand upon LXXLL binding to ER as recently reported *in vitro* (39). Alternatively, translocation of the LXXLL-containing peptide or GRIP1 from ER to another protein that resides in the same intranuclear position as ER could explain why the LXXLL-containing peptides and GRIP1 remain localized for prolonged periods of time after subsequent antagonist challenge.

The ligand specificity and temporal characteristics of intranuclear recruitment of ERα with each ligand indicated that, in the cellular environment, distinct conformations of ER are formed in response to E_2 and each SERM (7, 10). Recruitment was measured as a function of the percentage of cells responding to each ligand. The underlying basis for the cell-to-cell variability in recruitment remains to be described but may be responsible for the previous observation that dose-dependent transcriptional activation by a nuclear receptor ligand arises through an increase in the proportion of cells responding to the ligand rather than an equivalent, incremental increase in all cells (40).

The different abilities of E_2, tamoxifen, and raloxifene to promote ERα colocalization of the α/βV peptide, the class I LXXLL peptide, and GRIP1 provided dramatic evidence for the differing cellular and molecular properties of these clinically useful ligands. The E_2- and tamoxifen-induced recruitment of GRIP1 to the intranuclear location of ERα (Figs. 6 and 7) also contrasted with recruitment of related cofactor SRC-1a, which responded only to E_2, and not tamoxifen (27). This difference may be attributable to cell type or other experimental differences between laboratories, or to different ligand specificities for related cofactors in the context of the living cell. Nevertheless, the detection of these differences in living cells may prove useful in dissecting the differing clinical properties of E_2, tamoxifen, and raloxifene in different tissues (16, 18, 41, 42). The ability to quantify these changes on a pixel level (Fig. 4B) provide a first indicator that automated equipment can be developed for the high throughput measurement of ligand-specific effects on intranuclear recruitment and dissociation in living cells.

Recently, it was shown that the reticular intranuclear distribution of estrogen, SERM, and antiestrogen-bound ERα paralleled the tight binding of ERα to the nuclear matrix and that one ER-interacting factor, SRC-1a, was corecruited to the nuclear matrix via the ligand-bound ER (27). The results presented here suggest that other ER-interacting complexes may be similarly recruited to the nuclear matrix compartment upon ER binding to different ligands and that each ligand promotes the recruitment of specific nuclear receptor-interacting peptides and proteins (Table 1) with unique temporal kinetics (Figs. 4, 5, and 7). The ligand-regulated association of ER and ER-interacting complexes with the nuclear matrix is intriguing given the historical association of transcription markers and enhancer/promoter sequences with the nuclear matrix (43, 44). The nuclear matrix may aid the organization of transcriptionally competent chromosomal domains (45) but a decisive correlation of nuclear matrix association with transcriptional activation or repression remains to be established (46).

Thus, we demonstrated that recruitment of ER-interacting factors to the intranuclear position of ERα is differentially regulated by the nature of the interacting sequence and the type of ligand. The complex temporal kinetics and ligand specificities of the association of ERα and its cofactors illustrated a variety of possible responses of ERα to ligand addition for which the intranuclear colocalization assay provided a direct read-out *in vivo*. Other methods currently used to detect ER-peptide or cofactor interactions rely on various *in vitro* binding assays or on two-hybrid assays in cells. The advantage of the intranuclear colocalization assay is that it is an *in vivo* assay in which direct and indirect interactions of ER with specific peptide of cofactor targets are readily measured in real time. Therefore, the intranuclear colocalization assay allows the intracellular actions of each ligand to be dissected in unprecedented detail. The availability of many more ER-interacting peptides and cofactors (6, 7, 12–14, 20, 47) will permit the detection of an even more expanded series of ER activities and may also facilitate the identification of novel ligands that induce specific subsets of cofactor interactions with ER or other nuclear receptors. Such novel ligands could be used to probe for the specific molecular events involved in nuclear receptor regulation of different genes and may even provide a rapid means for the identification of compounds with improved specificity for hormone replacement therapies.

MATERIALS AND METHODS

Expression Vectors

The cDNA encoding the BFP Y66H, Y145F variant of GFP (28) or the cDNA encoding RFP (CLONTECH Laboratories, Inc. Palo Alto, CA) were fused in frame to the carboxy terminus of human ER and placed under the control of the cytomegalovirus promoter in the previously described BFP expression vector (35). The EGFP cDNA (CLONTECH Laboratories, Inc.), modified to include the SV40 nuclear localization signal (NLS) at its carboxy terminus, was inserted into the pTRE "Tet-On" expression plasmid (CLONTECH Laboratories, Inc.). Because of its small size, the modified EGFP-NLS remained distributed throughout the cytoplasm and nucleus when expressed. LXXLL (12) and α/βV (13) ER-interacting peptides were fused in frame to the carboxy terminus of EGFP-NLS in the pTRE expression plasmid. The αII (13) peptide was fused to the carboxy terminus of EGFP-NLS in the pEGFP-C3 vec-

tor (CLONTECH Laboratories, Inc.). The representative class I, class II, and class III LXXLL peptide sequences are from the D2, D47, and F6 peptides isolated in Ref. 12. Native GRIP1 and GRIP1 containing mutations in which ER-interacting, LXXLL boxes II and III (5) were mutated to LXXAA were appended to the carboxy terminus of GFP in the EGFP-C2 vector (CLONTECH Laboratories, Inc.).

Transfection

GHFT1–5 cells were grown in a 1:1 mixture of phenol red-free Ham's F12-DMEM containing estrogen-free 10% newborn calf serum. The cells were harvested and transfected by electroporation as described previously (35, 48) with 10 μg of the cytomegalovirus (CMV)-ERα-BFP or CMV-ERα-RFP expression vector, 10 μg of pEGFP-GRIP1 or pEGFP-GRIP1-ΔLXXLL, and 5 μg of pEGFP-αII or 3 μg of the pTRE-GFP-LXXLL or pTRE-GFP-α/βV expression vectors. pUHG17-1 (1.2 μg), which expresses the tetracycline repressor/VP16 activator (49) used to regulate expression of the pTRE plasmid, was cotransfected with the pTRE-GFP-LXXLL or pTRE-GFP-α/βV expression vectors. The transfected cells were plated onto coverslips and grown in estrogen-free media. Doxycycline (5 μg/ml) was added to the media to induce the Tet-On promoter except in Fig. 3B in which concentrations of doxycycline were varied from 0 to 15 μg/ml. One day after transfection, ER ligands were added at the indicated concentrations and imaged 24 h later (Figs. 2–6). For the E_2 time course experiments (Figs. 4C and 7), 10^{-8} M E_2 was added at the indicated time before imaging on the second day after transfection. For the ICI 182,780 antagonism time courses, cells were treated with 10^{-7} M tamoxifen (Fig. 8A) or 10^{-9} M E_2 (Fig. 8, B and C) for 24 h followed by addition of 10^{-6} M ICI 182,780 at the indicated times before imaging.

Microscopy and Image Analysis

After addition of ligand or ethanol control vehicle, fluorescence images from the transfected cells were acquired with a Axioplan microscope equipped with a 63×-oil immersion objective lens (Carl Zeiss, Thornwood, NY). Single-cell recordings of cells grown in chamber slides were obtained on an IX-70 inverted microscope (Olympus Corp., Lake Success, NY) and analyzed with Metamorph (Universal Imaging Corp., West Chester, PA) colocalization software. Dual color imaging using Hoechst and fluorescein isothiocyanate filter sets or GFP and rhodamine filter sets (Chroma Technology Corp., Brattleboro, VT) selectively distinguished blue from green fluorescence and green from red fluorescence, respectively. Appropriate controls in which ERα-BFP, ERα-RFP, or each GFP-peptide or GFP-GRIP were expressed individually ensured a lack of fluorescence bleedthrough between the channels. Grayscale images of the cells were obtained using a Xillix microscope (Carl Zeiss) or Hamamatsu ORCA microscope (Olympus Corp.) cooled CCD cameras. The digital images were background-subtracted and then converted to red-green-blue (RGB) images by assigning the GFP signal to the green channel, BFP signals to the blue channel, and RFP signals to the red channel of RGB digital images. Integration times and image processing were kept constant within each set of experiments.

Acknowledgments

We thank and Drs. Paul Webb and Peter Kushner (University of California, San Francisco) for helpful discussion, Drs. Tom Scanlon (UCSF) and A. E. Wakeling (Zeneca Pharmaceuticals) for the kind gifts of raloxifene and ICI 182,780, respectively, and Bill Hyun (UCSF) for expert microscopy advice.

Received June 8, 2000. Revision received August 30, 2000. Accepted September 11, 2000.

Address requests for reprints to: Dr. Fred Schaufele, Metabolic Research Unit, University of San Francisco, 513 Parnassus, HSW 1119, San Francisco, California 94122.

This work was supported by American Cancer Society Grant RPG-94-028-TBE, NIH Grant DK-54345, and the UCSF Academic Senate Committee on Research to F.S., by NIH Grant DK-48807 to D.P.M., and by US Army Grant DAMD17-99-1-9173 to C.-Y.C.

*J.D.B. has propietary interests in, and serves as a consultant and Deputy Director to, Karo Bio AB, which has commercial interests in this area of research.

REFERENCES

1. Tsai MJ, O'Malley BW 1994 Molecular mechanisms of action of steroid/thyroid receptor superfamily members. Annu Rev Biochem 63:451–486
2. Ribeiro RC, Apriletti JW, West BL, Wagner RL, Fletterick RJ, Schaufele F, Baxter JD 1995 The molecular biology of thyroid hormone action. Ann NY Acad Sci 758:366–389
3. Katzenellenbogen JA, O'Malley BW, Katzenellenbogen BS 1996 Tripartite steroid hormone receptor pharmacology: interaction with multiple effector sites as a basis for the cell- and promoter-specific action of these hormones. Mol Endocrinol 10:119–131
4. Heery DM, Kalkhoven E, Hoare S, Parker MG 1997 A signature motif in transcriptional co-activators mediates binding to nuclear receptors. Nature 387:733–736
5. Ding XF, Anderson CM, Ma H, Hong H, Uht RM, Kushner PJ, Stallcup MR 1998 Nuclear receptor-binding sites of coactivators glucocorticoid receptor interacting protein 1 (GRIP1) and steroid receptor coactivator 1 (SRC-1): multiple motifs with different binding specificities. Mol Endocrinol 12:302–313
6. Darimont BD, Wagner RL, Apriletti JW, Stallcup MR, Kushner PJ, Baxter JD, Fletterick RJ, Yamamoto KR 1998 Structure and specificity of nuclear receptor-coactivator interactions. Genes Dev 12:3343–3356
7. Shiau AK, Barstad D, Loria PM, Cheng L, Kushner PJ, Agard DA, Greene GL 1998 The structural basis of estrogen receptor/coactivator recognition and the antagonism of this interaction by tamoxifen. Cell 95:927–937
8. Danielian PS, White R, Lees JA, Parker MG 1992 Identification of a conserved region required for hormone dependent transcriptional activation by steroid hormone receptors. EMBO J 11:1025–1033
9. Feng W, Ribeiro RC, Wagner RL, Nguyen H, Apriletti JW, Fletterick RJ, Baxter JD, Kushner PJ, West BL 1998 Hormone-dependent coactivator binding to a hydrophobic cleft on nuclear receptors. Science 280:1747–1749
10. Brzozowski AM, Pike AC, Dauter Z, Hubbard RE, Bonn T, Engström O, Ohman L, Greene GL, Gustafsson JA, Carlquist M 1997 Molecular basis of agonism and antagonism in the oestrogen receptor. Nature 389:753–758
11. Webb P, Nguyen P, Shinsako J, Anderson C, Feng W, Nguyen MP, Chen D, Huang SM, Subramanian S, McKinerney E, Katzenellenbogen BS, Stallcup MR, Kushner PJ 1998 Estrogen receptor activation function 1 works by binding p160 coactivator proteins. Mol Endocrinol 12:1605–1618
12. Chang C-Y, Norris JD, Gron H, Paige LA, Hamilton PT, Kenan DJ, Fowlkes D, McDonnell DP 1999 Dissection of the LXXLL nuclear receptor-coactivator interaction motif using combinatorial peptide libraries: discovery of peptide antagonists of estrogen receptors α and β. Mol Cell Biol 19:8226–8239
13. Norris JD, Paige LA, Christensen DJ, Chang CY, Huacani MR, Fan D, Hamilton PT, Fowlkes DM, McDonnell DP 1999 Peptide antagonists of the human estrogen receptor. Science 285:744–746

14. Paige LA, Christensen DJ, Grøn H, Norris JD, Gottlin EB, Padilla KM, Chang CY, Ballas LM, Hamilton PT, McDonnell DP, Fowlkes DM 1999 Estrogen receptor (ER) modulators each induce distinct conformational changes in ER α and ER β. Proc Natl Acad Sci USA 96:3999–4004
15. Resche-Rigon M, Gronemeyer H 1998 Therapeutic potential of selective modulators of nuclear receptor action. Curr Opin Chem Biol 2:501–507
16. Jordan VC, Morrow M 1999 Tamoxifen, raloxifene, and the prevention of breast cancer. Endocr Rev 20:253–278
17. Gustafsson JA 1998 Therapeutic potential of selective estrogen receptor modulators. Curr Opin Chem Biol 2:508–511
18. Cummings SR, Eckert S, Krueger KA, Grady D, Powles TJ, Cauley JA, Norton L, Nickelsen T, Bjarnason NH, Morrow M, Lippman ME, Black D, Glusman JE, Costa A, Jordan VC 1999 The effect of raloxifene on risk of breast cancer in postmenopausal women: results from the MORE randomized trial. Multiple outcomes of raloxifene evaluation. JAMA 281:2189–2197
19. Colditz GA 1998 Relationship between estrogen levels, use of hormone replacement therapy, and breast cancer. J Natl Cancer Inst 90:814–823
20. McInerney EM, Rose DW, Flynn SE, Westin S, Mullen TM, Krones A, Inostroza J, Torchia J, Nolte RT, Assa-Munt N, Milburn MV, Glass CK, Rosenfeld MG 1998 Determinants of coactivator LXXLL motif specificity in nuclear receptor transcriptional activation. Genes Dev 12:3357–3368
21. Henttu PM, Kalkhoven E, Parker MG 1997 AF-2 activity and recruitment of steroid receptor coactivator 1 to the estrogen receptor depend on a lysine residue conserved in nuclear receptors. Mol Cell Biol 17:1832–1839
22. Htun H, Holth LT, Walker D, Davie JR, Hager GL 1999 Direct visualization of the human estrogen receptor α reveals a role for ligand in the nuclear distribution of the receptor. Mol Biol Cell 10:471–486
23. Htun H, Barsony J, Renyi I, Gould DL, Hager GL 1996 Visualization of glucocorticoid receptor translocation and intranuclear organization in living cells with a green fluorescent protein chimera. Proc Natl Acad Sci USA 93: 4845–4850
24. Fejes-Tóth G, Pearce D, Náray-Fejes-Tóth A 1998 Subcellular localization of mineralocorticoid receptors in living cells: effects of receptor agonists and antagonists. Proc Natl Acad Sci USA 95:2973–2978
25. Lim CS, Baumann CT, Htun H, Xian W, Irie M, Smith CL, Hager GL 1999 Differential localization and activity of the A- and B-forms of the human progesterone receptor using green fluorescent protein chimeras. Mol Endocrinol 13:366–375
26. van Steensel B, Brink M, van der Meulen K, van Binnendijk EP, Wansink DG, de Jong L, de Kloet ER, van Driel R 1995 Localization of the glucocorticoid receptor in discrete clusters in the cell nucleus. J Cell Sci 108:3003–3011
27. Stenoien DL, Mancini MG, Patel K, Allegretto EA, Smith CL, Mancini MA 2000 Subnuclear trafficking of estrogen receptor-a and steroid receptor coactivator-1. Mol Endocrinol 14:518–534
28. Heim R, Tsien RY 1996 Engineering green fluorescent protein for improved brightness, longer wavelengths and fluorescence resonance energy transfer. Curr Biol 6:178–182
29. Cavaillès V, Dauvois S, L'Horset F, Lopez G, Hoare S, Kushner PJ, Parker MG 1995 Nuclear factor RIP140 modulates transcriptional activation by the estrogen receptor. EMBO J 14:3741–3751
30. Yuan CX, Ito M, Fondell JD, Fu ZY, Roeder RG 1998 The TRAP220 component of a thyroid hormone receptor-associated protein (TRAP) coactivator complex interacts directly with nuclear receptors in a ligand-dependent fashion. Proc Natl Acad Sci USA 95:7939–7944
31. Rachez C, Lemon BD, Suldan Z, Bromleigh V, Gamble M, Näär AM, Erdjument-Bromage H, Tempst P, Freedman LP 1999 Ligand-dependent transcription activation by nuclear receptors requires the DRIP complex. Nature 398:824–828
32. Hong H, Kohli K, Garabedian MJ, Stallcup MR 1997 GRIP1, a transcriptional coactivator for the AF-2 transactivation domain of steroid, thyroid, retinoid, and vitamin D receptors. Mol Cell Biol 17:2735–2744
33. Hong H, Kohli K, Trivedi A, Johnson DL, Stallcup MR 1996 GRIP1, a novel mouse protein that serves as a transcriptional coactivator in yeast for the hormone binding domains of steroid receptors. Proc Natl Acad Sci USA 93:4948–4952
34. Oñate SA, Tsai SY, Tsai MJ, O'Malley BW 1995 Sequence and characterization of a coactivator for the steroid hormone receptor superfamily. Science 270: 1354–1357
35. Day RN 1998 Visualization of Pit-1 transcription factor interactions in the living cell nucleus by fluorescence resonance energy transfer microscopy. Mol Endocrinol 12:1410–1419
36. Chuang FM, West BL, Baxter JD, Schaufele F 1997 Activities in Pit-1 determine whether receptor interacting protein 140 activates or inhibits Pit-1/nuclear receptor transcriptional synergy. Mol Endocrinol 11:1332–1341
37. Webb P, Lopez GN, Uht RM, Kushner PJ 1995 Tamoxifen activation of the estrogen receptor/AP-1 pathway: potential origin for the cell-specific estrogen-like effects of antiestrogens. Mol Endocrinol 9:443–456
38. Chen H, Lin RJ, Xie W, Wilpitz D, Evans RM 1999 Regulation of hormone-induced histone hyperacetylation and gene activation via acetylation of an acetylase. Cell 98:675–686
39. Gee AC, Carlson KE, Martini PG, Katzenellenbogen BS, Katzenellenbogen JA 1999 Coactivator peptides have a differential stabilizing effect on the binding of estrogens and antiestrogens with the estrogen receptor. Mol Endocrinol 13:1912–1923
40. Ko MS, Nakauchi H, Takahashi N 1990 The dose dependence of glucocorticoid-inducible gene expression results from changes in the number of transcriptionally active templates. EMBO J 9:2835–2842
41. Osborne CK 1998 Tamoxifen in the treatment of breast cancer. N Engl J Med 339:1609–1618
42. Assikis VJ, Jordan VC 1997 Risks and benefits of tamoxifen therapy. Oncology 11:21–23
43. Bode J, Benham C, Knopp A, Mielke C 2000 Transcriptional augmentation: modulation of gene expression by scaffold/matrix-attached regions (S/MAR elements). Crit Rev Eukaryot Gene Expr 10:73–90
44. Stein GS, van Wijnen AJ, Stein JL, Lian JB, Pockwinse S, McNeil S 1998 Interrelationships of nuclear structure and transcriptional control: functional consequences of being in the right place at the right time. J Cell Biochem 70: 200–212
45. Brown K 1999 Nuclear structure, gene expression and development. Crit Rev Eukaryot Gene Expr 9:203–212
46. Pederson T 2000 Half a century of "the nuclear matrix." Mol Biol Cell 11:799–805
47. Northrop JP, Nguyen D, Piplani S, Olivan SE, Kwan ST-S, Go NF, Hart CP, Schatz PJ 2000 Selection of estrogen receptor β and thyroid hormone receptor β-specific coactivator-mimetic peptides using recombinant peptide libraries. Mol Endocrinol 14:623–633
48. Schaufele F 1996 CCAAT/enhancer-binding protein α activation of the rat growth hormone promoter in pituitary progenitor GHFT1-5 cells. J Biol Chem 271:21484–21489
49. Gossen M, Freundlieb S, Bender G, Müller G, Hillen W, Bujard H 1995 Transcriptional activation by tetracyclines in mammalian cells. Science 268:1766–1769
50. Schaufele F 1999 Regulation of estrogen receptor activation of the prolactin enhancer/promoter by antagonistic activation function-2-interacting proteins. Mol Endocrinol 13:935–945